

Evaluation of the Influence of MgO and La₂O₃ on the Fast Sintering of Mullite

Pollyane Márcia de Souto^{a*}, Romualdo Rodrigues Menezes^b,

Ruth Herta Goldschmidt Aliaga Kiminami^a

^aDepartment of Materials Engineering, Federal University of São Carlos – UFSCar,
Rod. Washington Luiz, km 235, CEP 13565-905, São Carlos, SP, Brazil

^bDepartment of Materials Engineering, Federal University of Campina Grande – UFCG,
Av. Aprígio Veloso, 882, Bodocongo, CEP 58429-900, Campina Grande, PB, Brazil

Received: January 19, 2014; Revised: January 12, 2015

The influence of MgO and La₂O₃ on the fast sintering of mullite was evaluated in this work. High-purity mullite was doped with MgO and La₂O₃, conventionally sintered, fast sintered, and microwave-sintered in rapid sintering cycles. The results showed that MgO and La₂O₃ strongly affected the densification of fast sintered samples; and only doped bodies reached high densities when fast sintered. However, the densification behavior of doped samples was dependent on the amount of sintering aids. MgO doped samples presented better densification behavior than La₂O₃ doped samples. Microwave-processed samples required a balance between power, time and amount of additives to obtain highly dense and homogenous microstructures.

Keywords: mullite, rapid sintering, sintering additives, MgO, La₂O₃

1. Introduction

Mullite (3Al₂O₃·2SiO₂) is one of the foremost ceramic materials and extensively studied crystalline phases in the Al₂O₃-SiO₂ binary system¹. Mullite has become a strong candidate material for advanced structural and functional ceramics in recent years, due to its outstanding properties of low thermal expansion, low thermal conductivity, and excellent creep resistance. Other favorable characteristics of mullite are suitable high temperature strength and excellent stability in harsh chemical environments².

However, the sintering of commercial mullite powders to produce dense compacts requires relatively high temperatures (>1600 °C) due to the strong covalent bonds in mullite and to the low interdiffusion rates of Si⁴⁺ and Al³⁺ within the mullite lattice³⁻⁵. Therefore, studies on the use of sintering aids to enhance the densification and sintering kinetics and lower the sintering temperature of mullite bodies are very important in order to produce high-strength low-cost bodies⁶.

The role of sintering additives has been attributed to the formation of liquid phase and to a reduction in viscosity of the glassy (or liquid) phase or to a reduction in mullite formation temperature in gel-derived powders, thereby leading to higher mobility of diffusing species⁷⁻¹¹.

Reports in the literature on studies involving mullite have focused on the nucleation of gel-derived mullites and doped mullites^{5,7,12-16} and on the conventional sintering of mullite compacts¹⁷⁻²⁰. Few researches have investigated the fast sintering behavior of mullite bodies²¹⁻²⁵, and even fewer studies^{26,27} have sought to ascertain the

influence of additives on the rapid sintering of mullite. In this context, some studies have observed benefits in the use of MgO^{9,18,28} and La₂O₃^{10,29-31} as sintering aids in the densification, microstructure evolution and strength of sintered mullite bodies.

Studies^{17,18} on the sintering of industrial mullites in the presence of magnesia as a sintering aid attributed the enhanced densification of doped mullite bodies to the formation of liquid phase. The amount of glassy phase significantly influenced the sinterability of mullite, which decreased when the amount of glassy phase was reduced. Similar to MgO, La₂O₃ also shows a strong glass forming tendency according to the La₂O₃-Al₂O₃-SiO₂ system^{10,32}.

However, as depicted before, few studies^{26,27}, and using only pulse electric current sintering, focused in the influence of these additives in the fast sintering of mullite, despite the advantages and benefits of the fast-firing technology.

The objective of fast firing is to enhance the ratio of the densification rate to the coarsening rate by rapidly reaching the sintering temperature. Because coarsening mechanisms commonly prevail over densification mechanisms at lower temperatures, it has been suggested that rapid heating to higher temperatures can favor the attainment of high density allied to fine grain size^{33,34}.

However, fast sintering involves some difficulties. The problem most often encountered in conventional fast firing is differential sintering, which causes differential densification, non-uniform microstructures and specimen cracking²⁴. In this context, microwave sintering has emerged in recent years as an alternative technique to overcome

*e-mail: pollyanesouto@yahoo.com.br

the problems of conventional fast sintering. Because it is a noncontact technique and the heat is transferred to the product via electromagnetic waves, large amounts of heat can be transferred into the material, minimizing the effects of differential sintering. In addition, it is believed³⁵ that densification processes during sintering can be accelerated by microwave energy, the microwave effect.

An analysis of data reported in the literature indicates that a basic understanding of the role of sintering additives in the fast sintering of mullite is still limited. Thus, this work aimed to evaluate the influence of MgO and La₂O₃ on the fast sintering of mullite.

2. Experimental Procedure

Commercial high-purity (99.5%) mullite (SCIMAREC MP40) powder was used in this work. Mullite powder is characterized elsewhere⁶. The chemical composition of mullite powder is similar to that of other commercial powders¹⁷, but it contains large amounts of ZrO₂ (0.27%) and TiO₂ (0.14%). The mullite used here had a D_{50} of about 1.5 μ m and a D_{10} and D_{90} of about 0.8 and 4.0 μ m, respectively. The powder's wide particle size distribution ranged from 0.3 to 7 μ m, with a high concentration of particles sizes of about 2 μ m.

Pure mullite powder with and without sintering aids (MgO and La₂O₃) was dispersed in an alcoholic medium by ball milling for 8h. Doped mullite was prepared by adding suitable amounts of magnesium oxide (MgO, > 98.5%, Merck) and lanthanum oxide (La₂O₃, 99.5%, Merck) to obtain additive concentrations of 0.5 wt.%, 1.0 wt.% and 2.0 wt.% of MgO (M) and La₂O₃ (L). The formulations containing 0.0 wt.%, 0.5 wt.%, 1.0 wt.% and 2.0 wt.% are identified here as Pure; 0.5M and 0.5L; 1M and 1L; and 2M and 2L, respectively. Disk-shaped samples (approximately 12 mm in diameter and 3 mm thick) were produced by unidirectional pressing under 40 MPa, followed by cold isostatic pressing (CIP) under 200 MPa. The average green density of the compacted disks was approximately 58% of the theoretical density, as determined from their dimensions and weights. Powder compacts of pure and 2% MgO doped mullite of approximately 38 mm in diameter and 5 mm thick were also produced and are identified as Pure38D and 2M38D.

Powder compacts were sintered from 1400 °C to 1600 °C with a soaking time of 120 min and a heating rate of 5 °C/min in conventional sintering processes. Samples were sintered at 1600 °C for 30min using heating rates of 40, 60 and 80 °C/min in rapid firing processes. Samples were sintered in a microwave furnace (multimode cavity) at 2.45GHz (Cober Electronics, MS6K), using susceptor materials as auxiliary heating elements, in rapid sintering cycles. Details of this sintering assembly are given elsewhere²⁴. Input power ranging from 0.9 to 2.4 kW and sintering times of up to 40 min were used in the microwave fast sintering processes. The cooling cycles of fast sintering and microwave sintering were not controlled, but the entire sintering (heating and cooling) cycle took < 1.5h in both processes.

The densities of sintered samples were determined by the water-immersion technique using the Archimedes

method. X-ray diffraction analysis was performed using CuK α radiation (40 kV and 40mA as working conditions) (Siemens D-500) to identify the presence of MgO or La₂O₃ related phases after the sintering process. Scanning electron microscopy (SEM) (PHILIPS, models XL30-FEG and XL30-TMP) was used to analyze the microstructural evolution. SEM samples were prepared according to the standard ceramographic techniques (cross sections of samples were polished and thermally etched). Grain sizes were measured using the linear-intercept technique and a stereographic correction factor of 1.56 was used. At least 600 grains were measured in each region.

3. Results and Discussion

Densities of conventionally sintered mullite (pure and doped) are shown in Figure 1. Sintering pure mullite up to 1550°C did not significantly increase the density of the compacts. At 1600°C, the density of pure mullite was approximately 90%. The addition of MgO and La₂O₃ favors the densification of mullite bodies, and all the doped samples presented higher densities than the pure mullite, which is consistent with reports in the literature^{9,10,18,30,31}. MgO enhanced the final density of mullite bodies considerably. At 1500°C, the addition of 1.0 wt.% and 2.0wt.% of MgO increased the density to values exceeding 97%. Similar additions of La₂O₃ increased the density up to only 87% and 92%, respectively, at 1500 °C. At 1600 °C, both additives effectively improved the densities, and additions of only 0.5% increased the density to values of about 96%. The mechanism of densification in mullite is grain boundary mass transport or diffusion, and the densification rates are essentially controlled by the presence of a liquid film². Thus, higher densities of doped mullite bodies have been attributed to the presence of liquid phase at sintering temperature, resulting from the addition of additives^{6,9,10}.

The density of pure mullite decreased considerably as the heating rate rose (Figure 2). This is probably due to need of mullite of long times for diffusion and densification. MgO doped samples, whose density did not decrease with the heating rate, reached densities similar to the highest ones

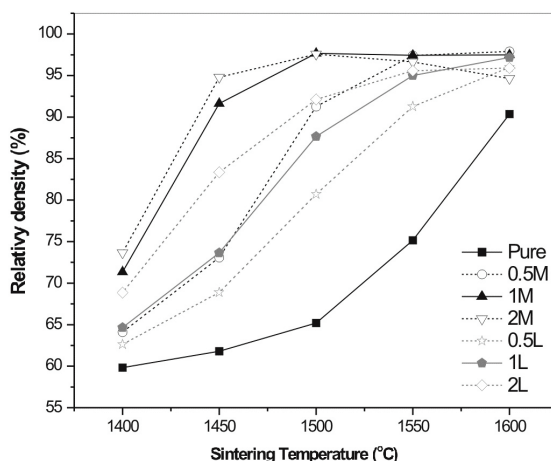


Figure 1. Relative density of conventionally sintered samples.

attained in conventional sintering (Figure 1). The addition of a mere 0.5% of MgO favored 98% densification in mullite bodies, despite the fast heating rates. Samples doped with 0.5 and 1% of La_2O_3 showed a reduction in densities in response to the increase in heating rates, decreasing from 96-97% to approximately 89% and 94%, respectively. However, the samples containing 2% of La_2O_3 behaved similarly to MgO doped samples, i.e., their density was not affected by fast firing. Doped bodies presented higher densities than pure mullite bodies at all the heating rates applied here. This may be attributed to the presence of liquid phase in these bodies during sintering, which improved the mobility of diffusing species favoring densification

Figure 3 shows the densities of microwave-sintered mullite. The densities of pure mullite did not change significantly when microwave-heated for 20min, and increased by up to 80% when microwave-sintered for 30 and 40 min. This value is lower than that achieved in conventional sintering, but is similar to the values attained at high heating rates (Figure 2). The power levels and sintering times applied in this study appeared to be insufficient for pure mullite to reach the critical temperature and couple efficiently with microwaves, which is necessary for fast sintering. This difficulty in microwave heating is the result of the very low dielectric loss factor of mullite, which requires very high temperatures for efficient coupling with microwaves.

Power levels of 0.9 and 1.2kW did not improve the densities of doped samples in any of the sintering times employed here. This may be attributed to insufficient energy (power and time) to raise the temperature of the samples and develop a densification process using microwave energy. However, at higher power levels, doped mullite achieved densities of approximately 97% in heating cycles of only 20 minutes. Doped bodies will develop liquid phase with heating, and this liquid phase increases the bodies' dielectric loss and hence their microwave absorption characteristics. Moreover, liquid phase is heated selectively, which increases

its temperature and decreases its viscosity, improving even more the diffusion and densification mechanisms.

Microwave fast-sintered bodies were devoid of cracks, which is a reliable indicator of homogeneous distribution of temperature in the bodies. However, samples Pure38D and 2M38D presented some cracks when conventionally fast sintered at 80°C/min. This indicated that despite the improvement in the densification behavior in response to MgO doping, the conventional fast sintering process presented limitations as a function of sample size.

MgO doped samples presented better densification behavior than La_2O_3 doped mullite. MgO doped mullite achieved densities of around 95% at a power level of 1.8kW, while lanthanum doped bodies reached similar densities at a power of 2.4kW and longer sintering times. However, all the doped samples exhibited higher densities than those of pure bodies in all the processing conditions of this study.

Pure samples and bodies containing 0.5 and 1.0% of sintering aids presented only mullite as crystalline phase after conventional sintering, fast sintering and microwave fast heating, according to the X-ray diffraction analysis. La_2O_3 or La_2O_3 related compounds were not observed in samples doped with 2.0%, irrespective of the processing conditions employed.

A change in mullite composition and related silica or alumina segregation is a phenomenon that occurs during high temperature processing or applications. Changes in concentration are due to the fact that the stability field of mullite tends towards Al_2O_3 at temperatures higher than 1600 °C^{36,37}. This indicates that microwave firing did not reach temperatures higher than 1600 °C or the cycle time was insufficient to decompose the mullite, which explains why only mullite was observed in the XRD patterns of pure samples.

However, spinel and alumina were detected in 2M samples. Figure 4 shows the XRD patterns of pure mullite fired at 1600 °C, 2M conventionally sintered samples and 2M fast fired samples. 2M microwave-sintered samples

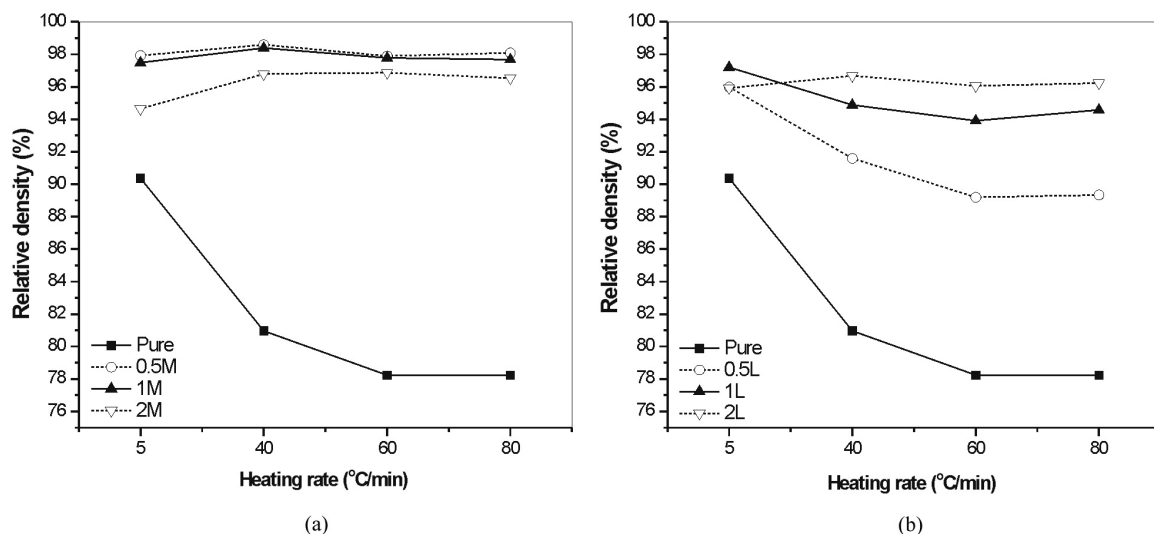


Figure 2. Relative density of fast sintered samples: a) MgO doped, and b) La_2O_3 doped.

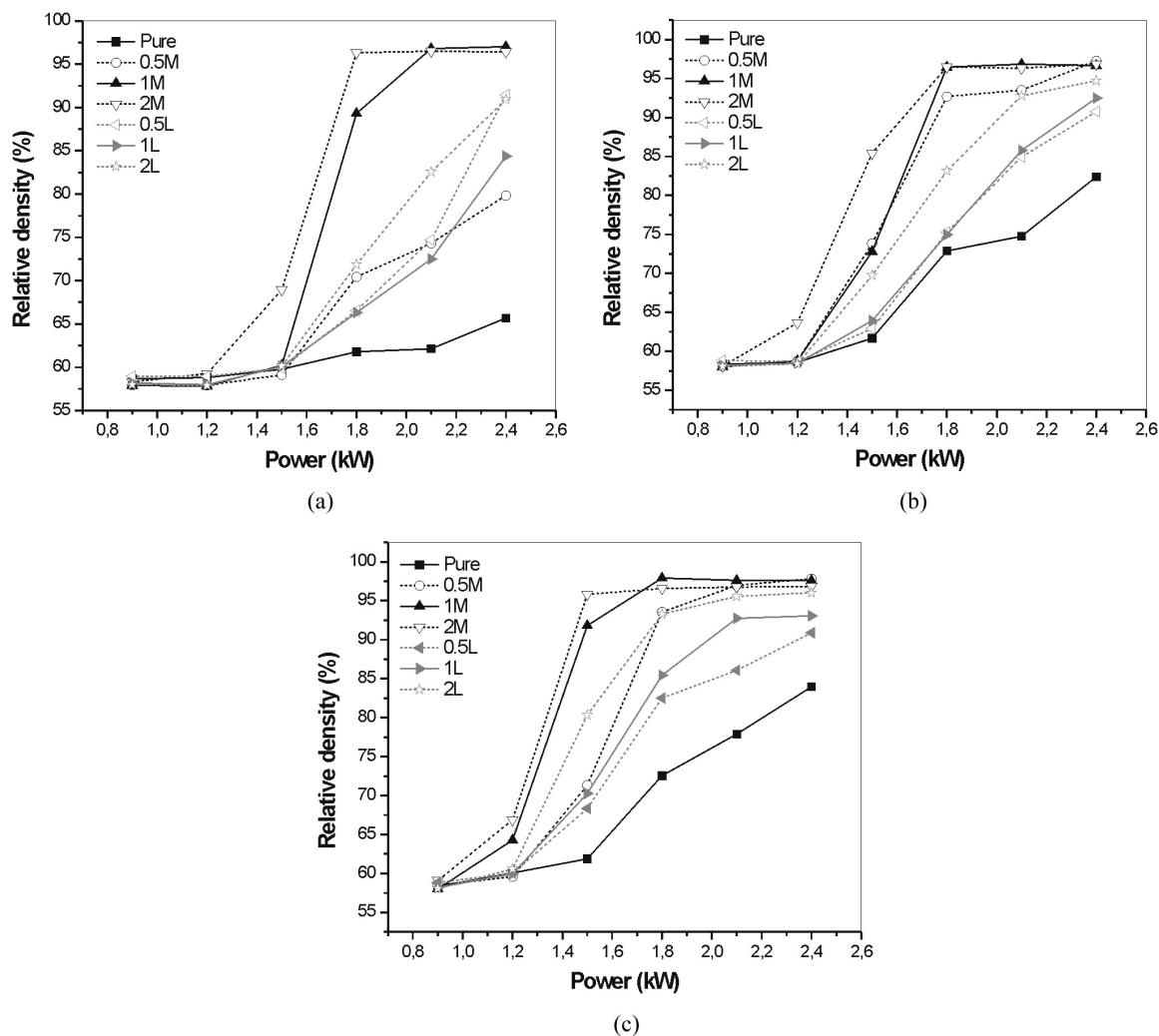


Figure 3. Relative density of samples microwave-sintered for: a) 20min, b) 30min and c) 40min.

also presented spinel and alumina when sintered for 40min, Figure 5.

Many authors^{9,17,18} have reported that sintering additives such as MgO, promote sintering in the presence of liquid phase, and that the addition of MgO increases the amount of glassy phase and induces partial dissolution of mullite¹⁸. It can be understood from the MgO–Al₂O₃–SiO₂ phase diagram that MgO addition can produce MgO–Al₂O₃ spinel at high temperatures. However, it should be emphasize that the analysis of the development of the crystalline phases depends on the system composition, the doping levels. In samples doped with 2.0 wt.% of MgO the final composition will enter the mullite-cordierite-sapphirine triangle, in which liquid forms at 1460 °C, and phases like cordierite or sapphirine could be expected after sintering (if there is enough cooling time). At high temperatures (higher than 1480 °C) and considering this equilibrium triangle the present phases are mullite, alumina and spinel. Temperatures lower than 1578 °C and regions with micro-heterogeneities richer in MgO will favor the formation of spinel. Thus, the presence of alumina and spinel observed in 2M samples is

a consequence of the system composition, of the processing temperatures and of the reaction kinetics during the cooling cycles.

In this sense, studies¹⁸ that analyzed the evolution of mullite bodies with increasing amounts of MgO as a sintering aid reported up to 11% and 25% of alumina in bodies containing 2 and 3 wt.% of MgO, respectively, after the sintering. On the other hand, when the sintering time or temperature is insufficient to cause high mullite dissolution, the amount of alumina in sintered bodies is expected to decrease. 2M bodies subjected to conventional fast sintering showed the presence of alumina. However, as mentioned earlier, with microwave sintering, alumina was detected only in samples processed for 40min. Thus, fast microwave processing of 2M samples for 20 and 30 min did not lead to high dissolution of mullite, despite the high densification achieved in these processing cycles. Low dissolution of mullite reduces the amount of glassy phase in bodies, which causes the development of microstructures containing prismatic mullite grains.

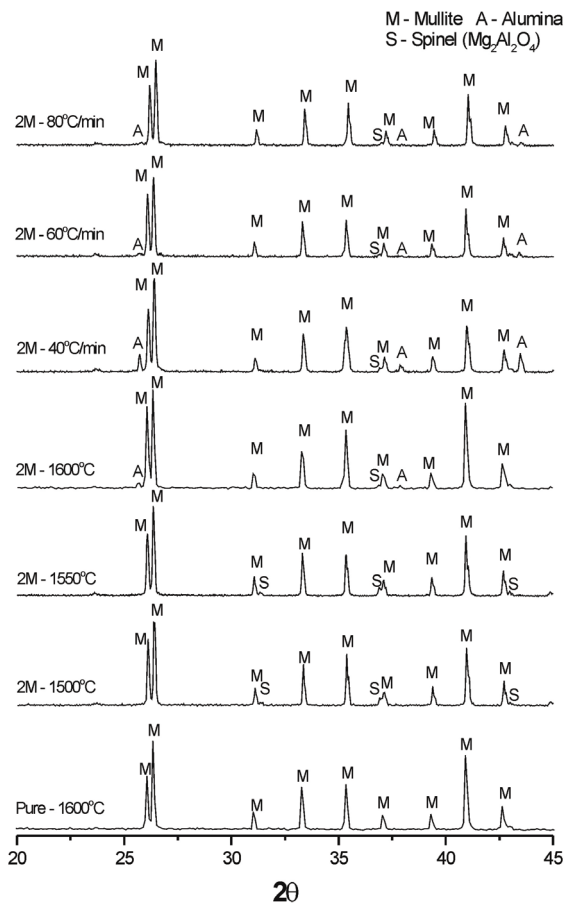


Figure 4. XRD patterns of the conventionally and fast sintered 2M samples.

Figures 6 and 7 depict SEM micrographs and Figures 7 and 8 show the grain size distribution of conventionally sintered doped samples. Mullite grain size increased as the amount of sintering aids increased, presenting a broader grain size distribution, irrespective of the sintering temperature. This effect was more pronounced in MgO doped samples. MgO doped samples presented heterogeneous microstructures with elongated grains after sintering at 1600 °C, whatever the amount of additive used. The La₂O₃ doped samples also displayed elongated grains, but presented less heterogeneous microstructures. Doped samples presented a broader grain size distribution (Figure 8 and 9) due to the presence of liquid phase. The literature^{2,38} indicates that mullite prepared in the absence of liquid phase invariably leads to an equiaxial (or quasi-equiaxial grain) microstructure, whereas the formation of elongated grains requires the presence of a liquid phase.

SEM micrographs of fast sintered samples (Figure 10 and 11) revealed the presence of elongated grains that were finer and more homogenous than those of samples conventionally sintered at 1600 °C. Increasing the heating rate resulted in more homogenous microstructures, with narrower grain size distributions, (Figures 8 and 9). Compared to conventionally sintered samples with similar

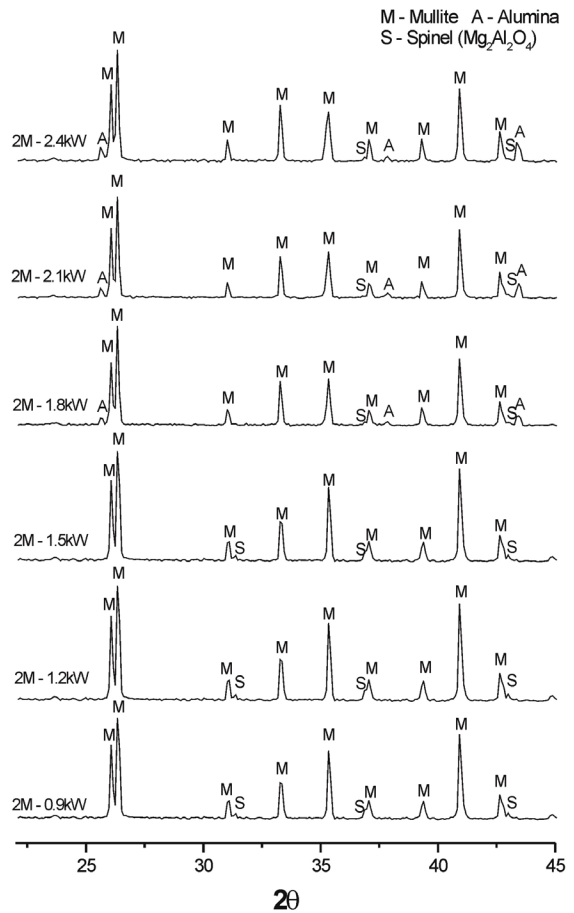


Figure 5. XRD patterns of 2M samples microwave fast sintered for 40min.

densities, MgO doped fast sintered samples showed a slightly smaller average grain size, while the average grain size of La₂O₃ doped bodies remained practically unchanged (Table 1). These results suggest that increasing the heating rate from 5 to 80°C/min when sintering doped bodies favors a narrower grain size distribution but not a reduction in grain size (comparing bodies with similar densities). The exception was the 2M sample, which exhibited a statistic significant decrease in average grain size (t test, $p < 0.001$) and different grain size distribution (Mann-Whitney test, $p < 0.001$) when the heating rate was increased from 40 to 80 °C/min. This behavior suggests that the fast sintering seems to be more effective in samples containing higher amount of MgO, favoring densification over coarsening mechanisms.

Figures 12 and 13 depict the microstructures of microwave-sintered samples. In general, the microwave-sintered samples exhibit greater homogeneity and narrower grain size distributions than those of conventionally sintered samples. However, the possible presence of liquid phase during sintering enhances the absorption of microwaves and promotes a rise in temperature and accelerates diffusion. This favors not only densification but also grain growth and the formation of elongated grains.

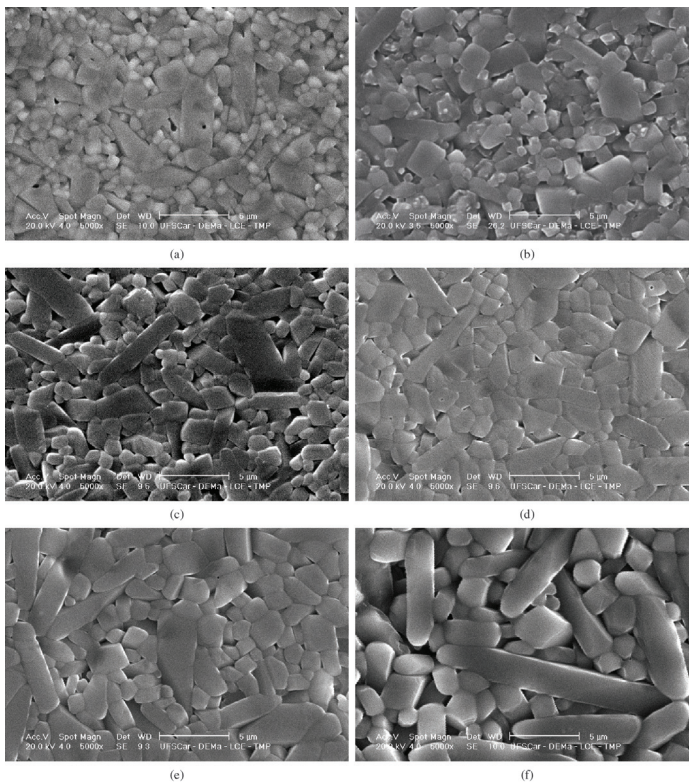


Figure 6. SEM micrographs of MgO doped samples conventionally sintered at 1500 °C/2h: (a) 0.5M, (b) 1M, (c) 2M; and at 1600 °C/2h (d) 0.5M, (e) 1M, (f) 2M.

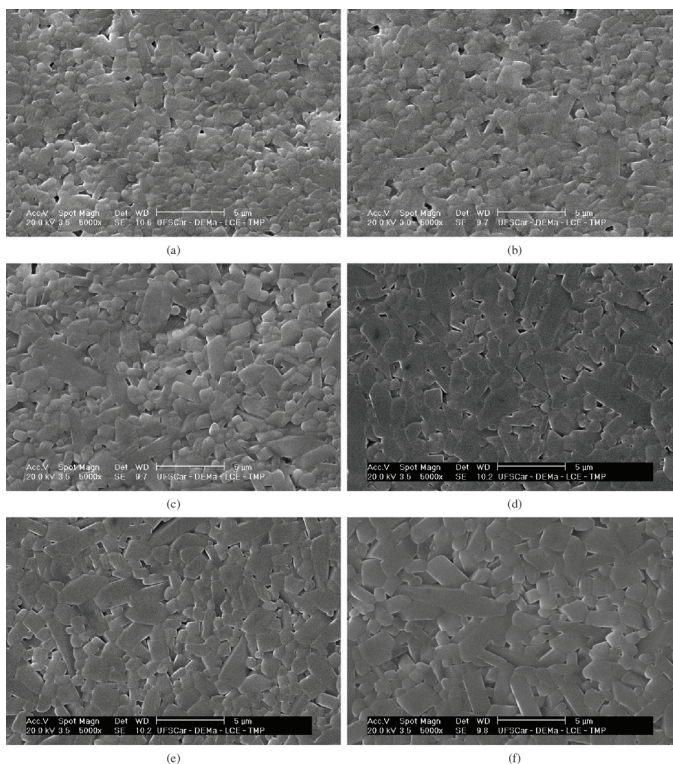


Figure 7. SEM micrographs of La₂O₃ doped samples conventionally sintered at 1500 °C/2h: (a) 0.5L, (b) 1L, (c) 2L; and at 1600 °C/2h (d) 0.5L, (e) 1L, (f) 2L.

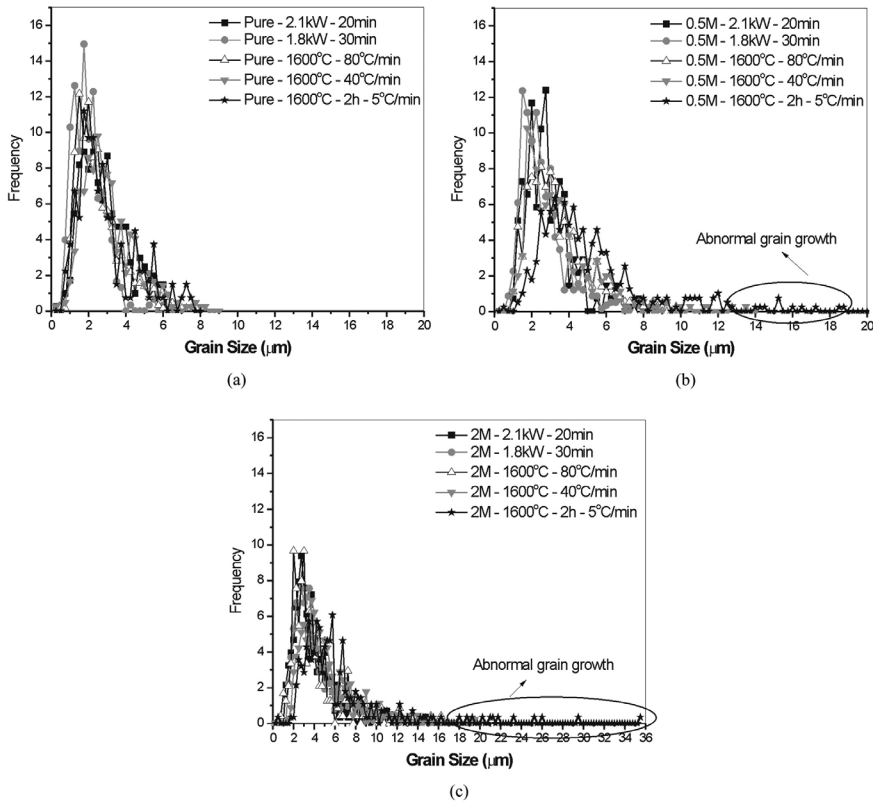


Figure 8. Grain size distribution of sintered MgO doped samples: (a) Pure, (b) 0.5M, (c) 2M.

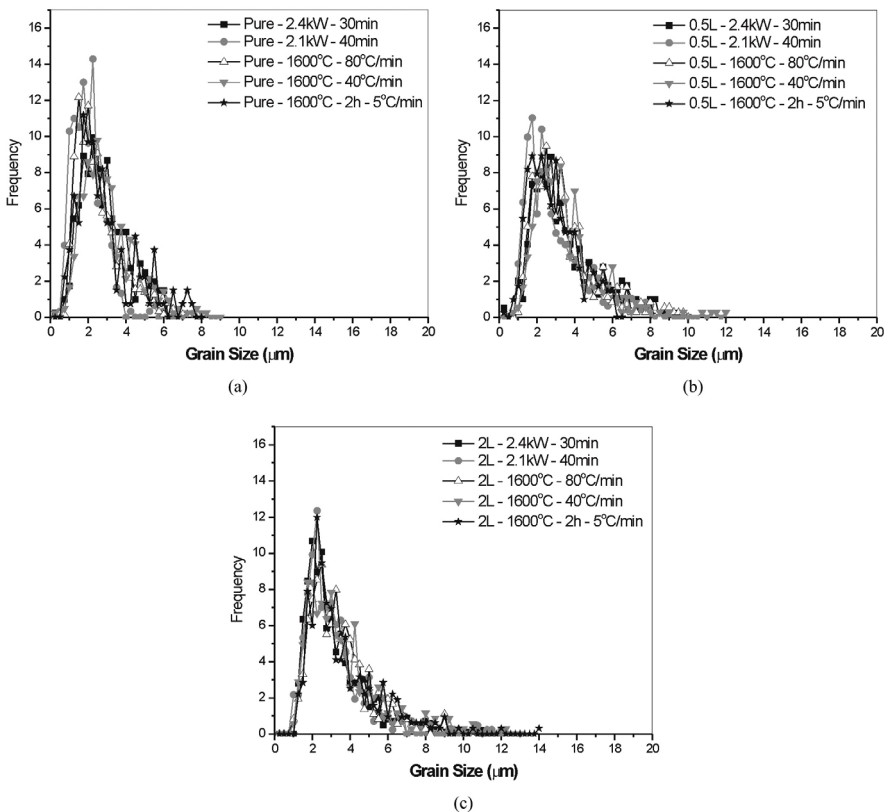


Figure 9. Grain size distribution of sintered La_2O_3 doped samples: (a) Pure, (b) 0.5L, (c) 2L.

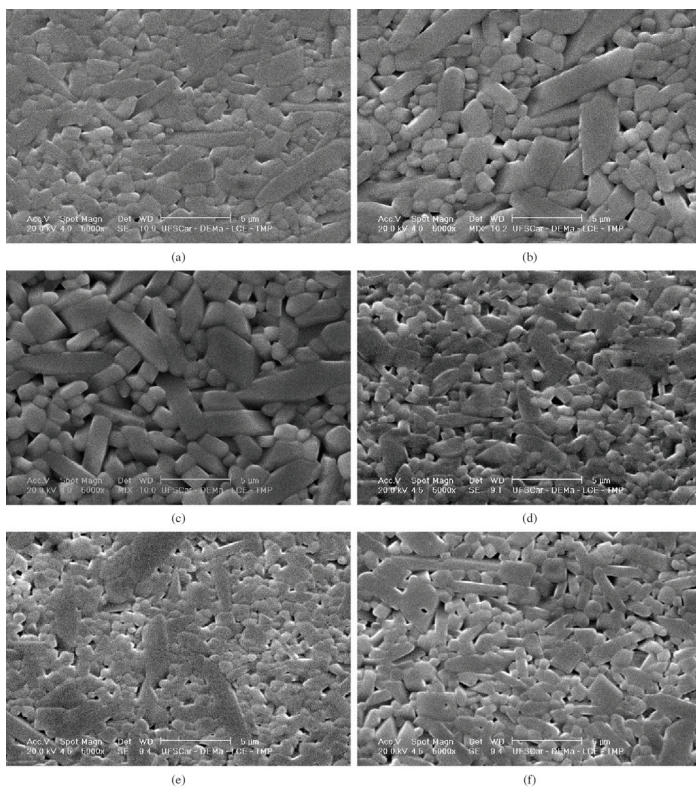


Figure 10. SEM micrographs of samples fast sintered at a heating rate of 40°C/min: (a) 0.5M, (b) 1M, (c) 2M, (d) 0.5L, (e) 1L, and (f) 2L.

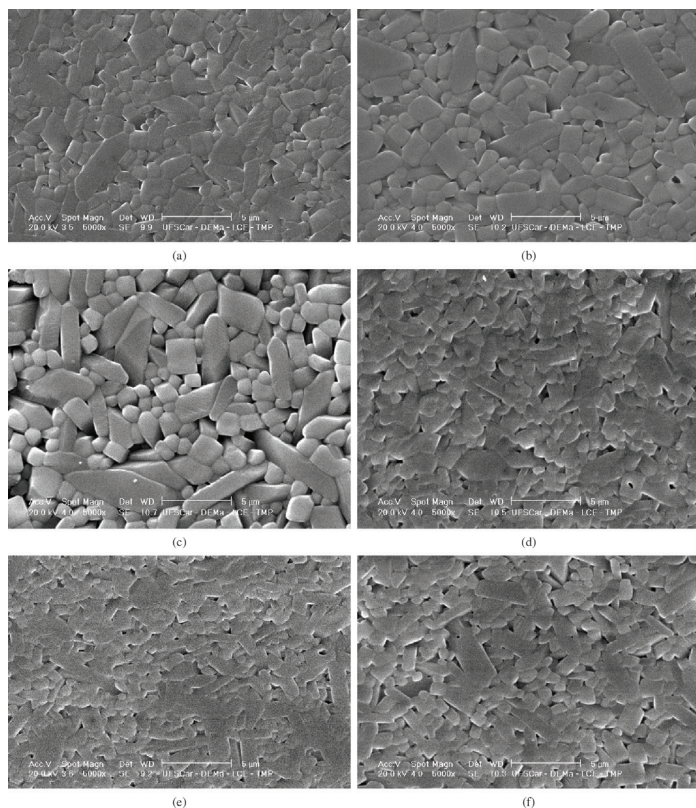
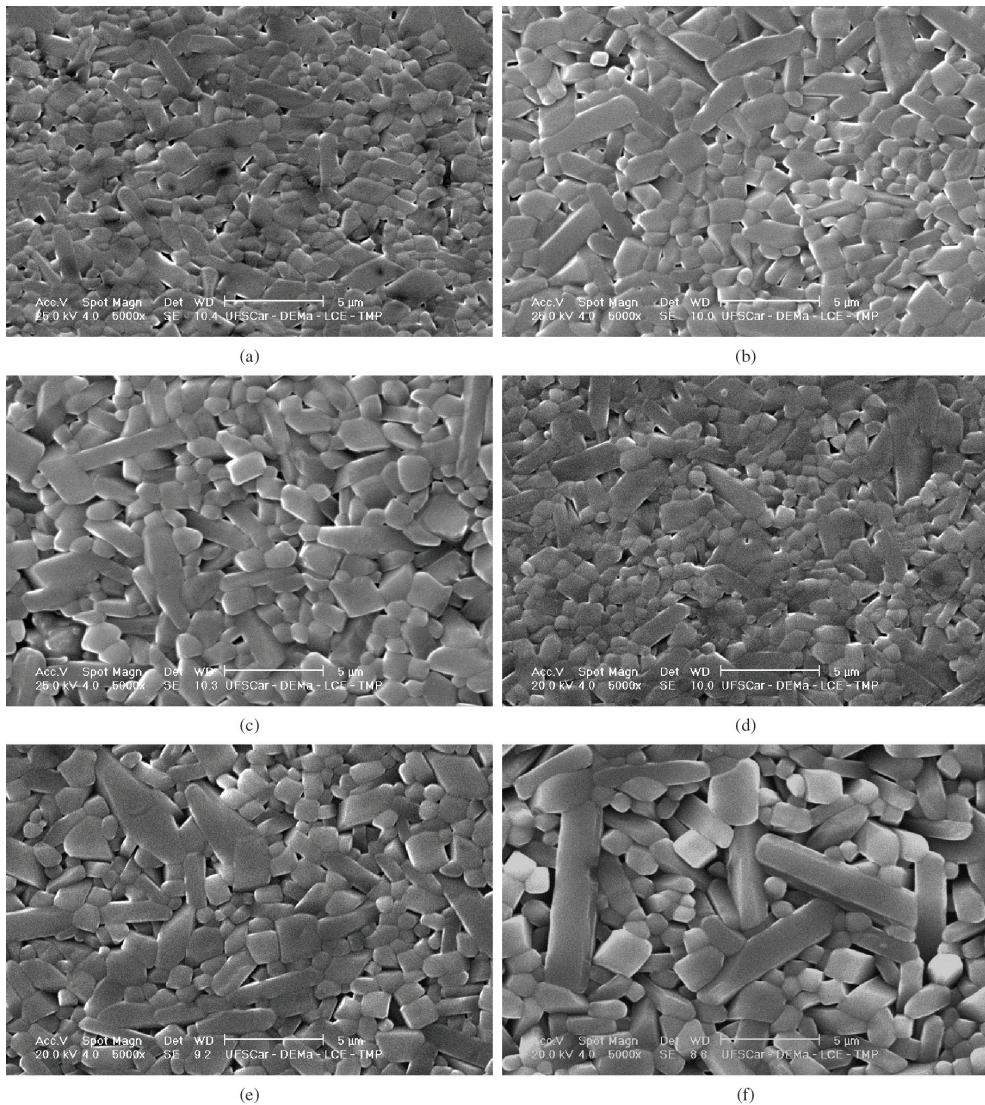


Figure 11. SEM micrographs of samples fast sintered at a heating rate of 80°C/min: (a) 0.5M, (b) 1M, (c) 2M, (d) 0.5L, (e) 1L, and (f) 2L.

Table 1. Average grain size of conventionally and fast sintered samples.

Sintering Condition		Average Grain Size (μm)						
		Pure	0.5M	1M	2M	0.5L	1L	2L
Conventional	1500 °C/2h	1.6 ± 0.9	3.4 ± 2.2	3.7 ± 2.9	4.0 ± 2.7	2.3 ± 1.5	2.8 ± 1.7	2.4 ± 1.5
	1550 °C/2h	1.6 ± 0.8	3.8 ± 2.2	4.4 ± 2.8	4.7 ± 2.6	2.4 ± 1.5	2.7 ± 1.5	3.1 ± 1.8
	1600 °C/2h	2.7 ± 1.5	4.9 ± 3.0	4.9 ± 3.2	6.3 ± 4.6	3.3 ± 1.7	3.3 ± 1.8	3.5 ± 2.0
Conventional Fast	40 °C/min	2.9 ± 1.4	3.4 ± 1.9	4.1 ± 2.7	5.0 ± 2.6	3.4 ± 1.7	3.2 ± 1.8	3.3 ± 1.8
	60 °C/min	2.7 ± 1.4	3.2 ± 1.6	4.0 ± 2.8	4.3 ± 2.3	3.1 ± 1.6	3.2 ± 1.9	3.5 ± 1.8
	80 °C/min	2.4 ± 1.2	3.2 ± 1.6	3.6 ± 2.1	3.7 ± 2.4	3.3 ± 1.7	3.1 ± 1.8	3.3 ± 1.6
Microwave	1.8kW/30min	1.8 ± 0.8	2.5 ± 1.3	3.0 ± 1.5	4.1 ± 2.3	2.8 ± 1.2	2.2 ± 1.1	2.6 ± 1.3
	1.8kW/40min	2.2 ± 1.2	3.3 ± 1.8	3.7 ± 2.1	4.5 ± 2.8	2.4 ± 1.2	2.6 ± 1.3	2.6 ± 1.3
	2.1kW/20min	2.6 ± 1.2	2.7 ± 1.3	3.2 ± 1.6	3.8 ± 2.1	2.7 ± 1.1	2.5 ± 1.2	2.6 ± 1.1
	2.1kW/40min	2.4 ± 1.2	3.3 ± 2.1	4.2 ± 2.5	5.3 ± 3.2	2.8 ± 1.6	2.8 ± 1.6	3.0 ± 1.7
	2.4kW/30min	2.7 ± 1.4	3.4 ± 1.9	4.3 ± 2.5	4.9 ± 3.0	3.4 ± 1.8	2.9 ± 1.7	3.2 ± 1.8
	2.4kW/40min	2.5 ± 1.0	3.6 ± 2.2	4.1 ± 2.7	4.8 ± 2.9	2.8 ± 1.2	4.9 ± 2.8	5.8 ± 3.3

**Figure 12.** SEM micrographs of MgO doped samples microwave-sintered at: 1.8kW/30min (a) 0.5M, (b) 1M, (c) 2M; and 1.8kW/40min (d) 0.5M, (e) 1M, (f) 2M.

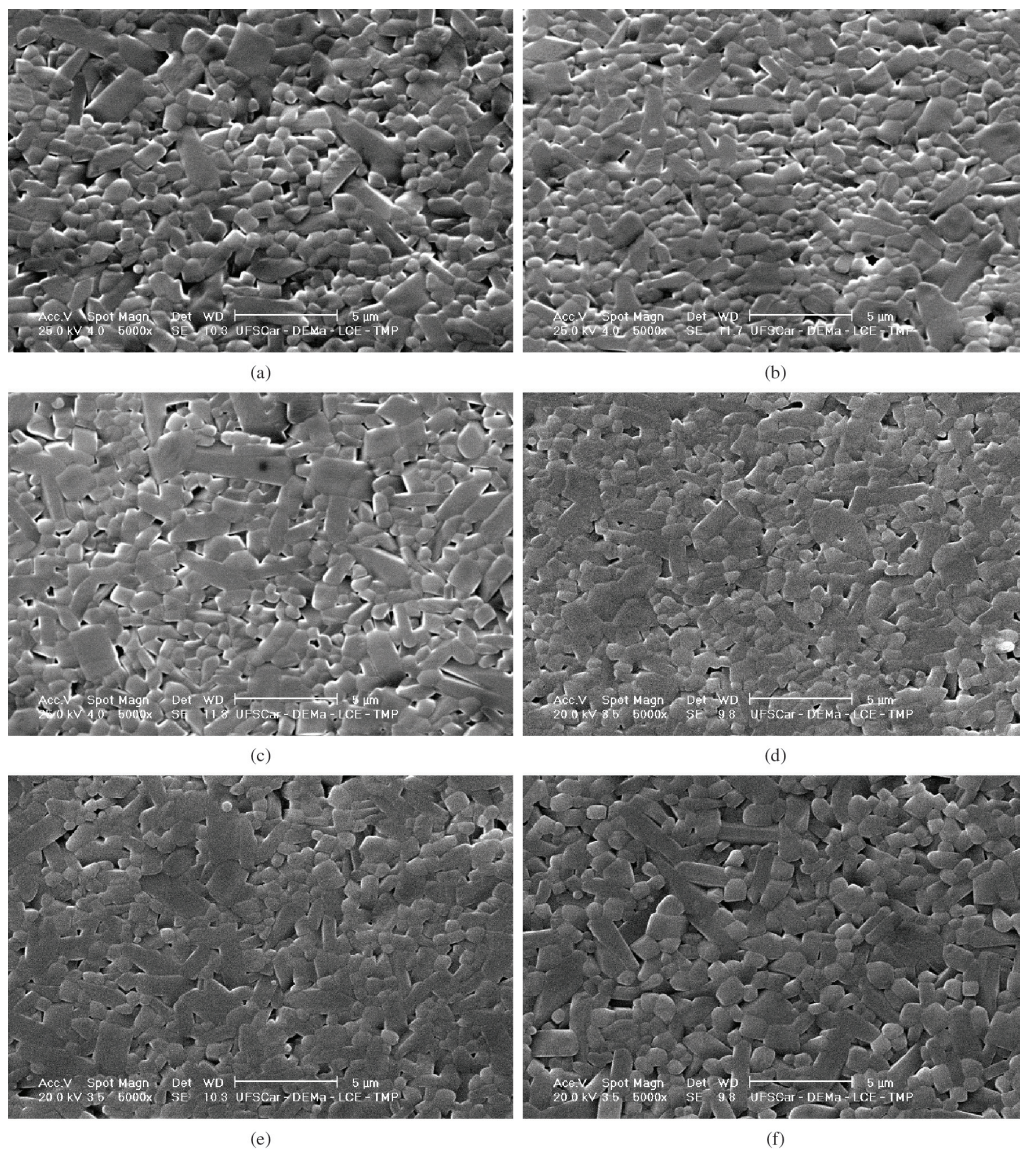


Figure 13. SEM micrographs of La₂O₃ doped samples microwave-sintered at: 2.1kW/30min (a) 0.5L, (b) 1L, (c) 2L; and 2.1kW/40min (d) 0.5L, (e) 1L, (f) 2L.

Thus, a balance must be achieved between the amount of additive, the power level and the sintering time in the microwave sintering process to attain not only high densities but also homogeneous microstructures. A good example of this requirement is the increase in sintering time from 30 to 40min at a power level of 1.8kW, which was applied to process MgO doped mullite (Figure 12). The longer sintering time led to a broader grain size distribution and increased the amount of elongated grains.

Microwave-sintered samples doped with La₂O₃ required higher power levels to reach densities similar to those of MgO doped bodies, as can be seen in Figure 3. This is due to the lower densification or heating behavior of La₂O₃ doped samples in microwave sintering. However, the use of an adequate sintering cycle results in more homogenous microstructures, with a smaller average grain size and narrower grain size distribution.

The microstructures of microwave-processed samples proved to be highly dependent on the sintering conditions, as mentioned earlier. Thus, according to the power level and heating time used, microstructures may be similar, finer or coarser than those achieved when conventionally fast sintering doped bodies.

Based on a comparison of the densities and microstructures of pure and doped mullite, the pure samples were found to present a more porous microstructure in all the analyzed conditions. This difference was more pronounced in fast firing cycles, with pure mullite bodies presenting significantly lower densification. The short time of fast sintering processes and the slow diffusion in mullite systems appeared to be the reasons for the difficulty in achieving densification of fast sintered pure mullite. The conclusions and results obtained here indicate that effective fast sintering of mullite bodies seems to be dependent on the use of liquid

phase-promoting additives. Moreover, in microwave fast sintering a liquid phase will also improve the coupling with microwaves, accelerating the densification process.

4. Conclusions

The influence of MgO and La₂O₃ on the fast sintering of mullite was investigated here. MgO and La₂O₃ exerted a marked influence on the densification process of fast sintered samples, and only the doped bodies achieved high densities when rapidly sintered. Fast sintering of mullite bodies seems to be highly dependent on the presence of some liquid phase-promoting additive. The microstructures of doped fast sintered bodies were more homogenous than those of conventionally sintered samples, but presented a similar

average grain size. The additives significantly improved mullite coupling with microwaves, and only doped bodies displayed high densities in microwave fast sintering. The microstructures of microwave-processed samples showed a strong dependence on the sintering conditions, and it was found that a balance is required between power, time and amount of additives to obtain highly dense and homogenous microstructures.

Acknowledgements

The authors gratefully acknowledge the Brazilian agencies FAPESP (proc. 07/59564-0) and CNPq (grants nos. 472638/2008-4, 303388/2009-9 and 308980/2012-3) for their financial support.

References

- Ebadzadeh T, Sarrafi MH and Salahi E. Microwave-assisted synthesis and sintering of mullite. *Ceramics International*. 2009; 35(8):3175-3179. <http://dx.doi.org/10.1016/j.ceramint.2009.05.013>.
- Schneider H and Komarneni S, editors. *Mullite*. Weinheim: Wiley-VCH Verlag GmbH & Co. KGaA; 2005. <http://dx.doi.org/10.1002/3527607358>.
- Burgos-Montes O, Moreno R, Colomer MT and Fariñas JC. Synthesis of mullite powders through a suspension combustion process. *Journal of the American Ceramic Society*. 2006; 89(2):484-489. <http://dx.doi.org/10.1111/j.1551-2916.2005.00771.x>.
- Baudin C and Moya JS. Influence of titanium dioxide on the sintering rate and microstructural evolution of mullite. *Journal of the American Ceramic Society*. 1984; 67:C130-C131.
- Rani DA, Jayaseelan DD and Gnanam FD. Densification behavior and microstructure of gel-derived phase-pure mullite in the presence of sinter additives. *Journal of the European Ceramic Society*. 2001; 21(12):2253-2257. [http://dx.doi.org/10.1016/S0955-2219\(00\)00328-9](http://dx.doi.org/10.1016/S0955-2219(00)00328-9).
- Souto PM, Menezes RR and Kiminami RHGA. Sintering of commercial mullite powder: Effect of MgO dopant. *Journal of Materials Processing Technology*. 2009; 209(1):548-553. <http://dx.doi.org/10.1016/j.jmatprotec.2008.02.029>.
- Hong SH, Cermignani W and Messing GL. Anisotropic grain growth in seeded and B₂O₃-doped diphasic mullite gels. *Journal of the European Ceramic Society*. 1996; 16(2):133-141. [http://dx.doi.org/10.1016/0955-2219\(95\)00144-1](http://dx.doi.org/10.1016/0955-2219(95)00144-1).
- She JH, Mechnich P, Schmucker M and Schneider H. Low-temperature reaction-sintering of mullite ceramics with an Y₂O₃ Addition. *Ceramics International*. 2001; 27(8):847-852. [http://dx.doi.org/10.1016/S0272-8842\(01\)00039-6](http://dx.doi.org/10.1016/S0272-8842(01)00039-6).
- Viswabaskaran V, Gnanam FD and Balasubramanian M. Effect of MgO, Y₂O₃ and Boehmite Additives on the Sintering Behaviour of Mullite formed from Kaolinite-Reactive Alumina. *Journal of Materials Processing Technology*. 2003; 142(1):275-281. [http://dx.doi.org/10.1016/S0924-0136\(03\)00577-6](http://dx.doi.org/10.1016/S0924-0136(03)00577-6).
- Kong LB, Zhang TS, Ma J, Boey F and Zhang RF. Mullite phase formation in oxide mixtures in the presence of Y₂O₃, La₂O₃ and CeO₂. *J. All. Comp*. 2004; 372(1-2):290-299. <http://dx.doi.org/10.1016/j.jallcom.2003.10.022>.
- Arellano-López AR, Meléndez-Martínez JJ, Cruse TA, Koritala RE, Routbort JL and Goretta KC. Compressive creep of mullite containing Y₂O₃. *Acta Materialia*. 2002; 50(17):4325-4338. [http://dx.doi.org/10.1016/S1359-6454\(02\)00264-1](http://dx.doi.org/10.1016/S1359-6454(02)00264-1).
- Hong SH and Messing GL. Anisotropic grain growth in diphasic-gel-derived titania doped mullite. *Journal of the American Ceramic Society*. 1998; 81(5):1269-1277. <http://dx.doi.org/10.1111/j.1151-2916.1998.tb02478.x>.
- Chakraborty AK and Das S. Al-Si spinel phase formation in diphasic mullite gels. *Ceramics International*. 2003; 29(1):27-33. [http://dx.doi.org/10.1016/S0272-8842\(02\)00084-6](http://dx.doi.org/10.1016/S0272-8842(02)00084-6).
- Sola ER, Estevan F and Alarcón J. Low-temperature Ti-containing 3:2 and 2:1 mullite nanocrystals from single-phase gels. *Journal of the European Ceramic Society*. 2007; 27(7):2655-2663. <http://dx.doi.org/10.1016/j.jeurceramsoc.2006.09.014>.
- Gridi-Bennadji F, Zimová J, Laval JP and Blanchart P. Mullite interaction with bismuth oxide from minerals and sol-gel processes. *Ceramics International*. 2010; 36(1):129-134. <http://dx.doi.org/10.1016/j.ceramint.2009.07.021>.
- Zhang G, Fu Z, Wang Y, Wang H, Wang W, Zhang J, et al. Boron-doped mullite derived from single-phase gels. *Journal of the European Ceramic Society*. 2010; 30(12):2435-2441. <http://dx.doi.org/10.1016/j.jeurceramsoc.2010.05.017>.
- Montanaro L, Tulliani JM, Perrot C and Negro A. Sintering of industrial mullites. *Journal of the European Ceramic Society*. 1997; 17(14):1715-1723. [http://dx.doi.org/10.1016/S0955-2219\(97\)00043-5](http://dx.doi.org/10.1016/S0955-2219(97)00043-5).
- Montanaro L, Perrot C, Esnouf C, Thollet G, Fantozzi G and Negro A. Sintering of industrial mullites in the presence of magnesia as a sintering aid. *Journal of the American Ceramic Society*. 2000; 83(1):189-196. <http://dx.doi.org/10.1111/j.1151-2916.2000.tb01169.x>.
- Ebadzadeh T. Formation of mullite from precursor powders: sintering, microstructure and mechanical properties. *Materials Science and Engineering A*. 2003; 355(1-2):56-61. [http://dx.doi.org/10.1016/S0921-5093\(03\)00049-2](http://dx.doi.org/10.1016/S0921-5093(03)00049-2).
- Chen Z, Zhang L, Cheng L, Xiao P and Duo G. Novel method of adding seeds for preparation of mullite. *Journal of Materials Processing Technology*. 2005; 166(2):183-187. <http://dx.doi.org/10.1016/j.jmatprotec.2004.07.105>.
- Gao L, Hong JS, Miyamoto H and De La Torre SE. Superfast densification of oxide ceramics by spark plasma sintering. *Journal of Inorganic Materials*. 1998; 13:18-22.
- Fang Y, Roy R, Agrawal DK and Roy DM. Transparent mullite ceramics from diphasic aerogels by microwave and

- conventional processings. *Materials Letters*. 1996; 28(1-3):11-15. [http://dx.doi.org/10.1016/0167-577X\(96\)00028-6](http://dx.doi.org/10.1016/0167-577X(96)00028-6).
23. Gahler A, Heinrich JG and Günster J. Direct laser sintering of Al₂O₃-SiO₂ dental ceramic components by layer-wise slurry deposition. *Journal of the American Ceramic Society*. 2006; 89(10):3076-3080. <http://dx.doi.org/10.1111/j.1551-2916.2006.01217.x>.
 24. Souto PM, Menezes RR and Kiminami RHGA. Microwave hybrid sintering of mullite powders. *American Ceramic Society Bulletin*. 2007; 86(1):9201-9206.
 25. Zhang G, Wang Y, Fu Z, Wang H, Wang W, Zhang J, et al. Transparent mullite ceramic from single-phase gel by spark plasma sintering. *Journal of the European Ceramic Society*. 2009; 29(13):2705-2711. <http://dx.doi.org/10.1016/j.jeurceramsoc.2009.04.012>.
 26. Sivakumar R, Jayaseelan DD, Nishikawa T, Honda S and Awaiji H. Influence of MgO on microstructure and properties of mullite-Mo composites fabricated by pulse electric current sintering. *Ceramics International*. 2001; 27(5):537-541. [http://dx.doi.org/10.1016/S0272-8842\(00\)00115-2](http://dx.doi.org/10.1016/S0272-8842(00)00115-2).
 27. Jayaseelan DD, Rani A, Anburaj DB and Ohji T. Pulse electric current sintering and microstructure of industrial mullite in the presence of sintering aids. *Ceramics International*. 2004; 30(4):539-543. <http://dx.doi.org/10.1016/j.ceramint.2003.09.005>.
 28. Viswabaskaran V, Gnanam FD and Balasubramanian M. Mullite from clay-reactive alumina for insulating substrate application. *Applied Clay Science*. 2004; 25(1-2):29-35. <http://dx.doi.org/10.1016/j.clay.2003.08.001>.
 29. Mitamura T, Kobayashi H, Ishibashi N and Akiba T. Effects of rare earth oxide addition on the sintering of mullite. *Journal of the Ceramic Society of Japan*. 1991; 99(1149):351-356. <http://dx.doi.org/10.2109/jcersj.99.351>.
 30. Wang W, Weng D and Wu XD. Structure evolution and thermal stability of La₂O₃-doped mullite fibers via sol-gel method. *Journal of Rare Earths*. 2012; 30(2):175-180. [http://dx.doi.org/10.1016/S1002-0721\(12\)60018-0](http://dx.doi.org/10.1016/S1002-0721(12)60018-0).
 31. Ji HP, Fang MH, Huang ZH, Chen K, Xu YG, Liu YG, et al. Effect of La₂O₃ additives on the strength and microstructure of mullite ceramics obtained from coal gangue and gamma-Al₂O₃. *Ceramics International*. 2013; 39(6):6841-6846. <http://dx.doi.org/10.1016/j.ceramint.2013.02.016>.
 32. Regiani I, Magalhães WLE, Souza DPF, Paiva-Santos CO and Souza MF. Nucleation and growth of mullite whiskers from lanthanum-doped aluminosilicate melts. *Journal of the American Ceramic Society*. 2002; 85(1):232-238. <http://dx.doi.org/10.1111/j.1551-2916.2002.tb00071.x>.
 33. Harmer MP, Brook RJ. Fast firing: microstructural benefits. *Transaction of the British Ceramic Society*. 1981; 80:147-148.
 34. Lin FJT, De Jonghe LC and Rahaman MN. Initial coarsening and microstructural evolution of fast-fired and MgO-doped Al₂O₃. *Journal of the American Ceramic Society*. 1997; 80(11):2891-2896. <http://dx.doi.org/10.1111/j.1551-2916.1997.tb03208.x>.
 35. Clark DE and Sutton W. Microwave processing of materials. *Annual Review of Materials Science*. 1996; 26(1):299-331. <http://dx.doi.org/10.1146/annurev.ms.26.080196.001503>.
 36. Klug FJ, Prochazka S and Doremus RH. Alumina-silica phase diagram in the mullite region. *Journal of the American Ceramic Society*. 1987; 70(10):750-759. <http://dx.doi.org/10.1111/j.1551-2916.1987.tb04875.x>.
 37. Fielitz P, Borchardt G, Mechnich P and Schmücker M. Kinetics of alumina segregation in mullite ceramics. *Journal of the European Ceramic Society*. 2008; 28(2):401-406. <http://dx.doi.org/10.1016/j.jeurceramsoc.2007.03.014>.
 38. Huang T, Rahaman MN, Mah T and Parthasarathay TA. Anisotropic grain growth and microstructural evolution of dense mullite above 1550°C. *Journal of the American Ceramic Society*. 2000; 83(1):204-210. <http://dx.doi.org/10.1111/j.1551-2916.2000.tb01171.x>.